A Lower Limb Phantom for Simulation and Assessment of Electromyography Technology

Bryan R. Schlink and Daniel P. Ferris, *Senior Member, IEEE*

***Abstract*— Electromyography signal processing approaches have traditionally been validated through computer simulations. Electromyography electrodes and systems are often not validated or have been validated on human subjects where there is no clear ground truth signal for comparison. We sought to develop a physical limb phantom for validation of electromyography hardware and signal processing approaches. We embedded pairs of wires within a conductive gelatin surrounding an artificial bone such that the antennae could broadcast identified ground truth signals. The ground truth signals can be simple sinusoids or more complex representations of muscle activity. With the phantom and surface electromyography electrodes, we were able to show varying levels of crosstalk between nearby recording electrodes as we altered the amplitude of the antennae signals. We were also able to induce motion artifacts in our recordings by lightly dropping the phantom on a surface while antennae broadcast signals. High-density electromyography recordings of the trials showed that traditional filtering techniques fail to fully eliminate relatively small motion artifacts. The results suggest that the electrical limb phantom could be a valuable tool for testing potential effects of muscle crosstalk and motion artifacts on different electromyography systems and signal processing approaches.**

***Index Terms*— Crosstalk, electromyography, lower limb, motion artifact, phantom, running, walking.**

I. Introduction

SURFACE electromyography (EMG) is a non-invasive method for quantifying the electrical activity of muscles with technical limitations [1], [2]. Signal crosstalk between neighboring muscles and motion artifacts are especially relevant when recording EMG during dynamic conditions, such as walking and running [3]. Crosstalk occurs when a surface electrode on one muscle records a signal from both the target muscle and one or more nearby muscles [3], [4]. The level of crosstalk depends on the size and location of the target muscles [5]. Surface EMG measurements from a target muscle may contain up to 30% of a non-target muscle's signal [6]. Motion artifacts can result from disturbance of the electrode and deformation of the skin beneath the electrode [7]. They are particularly large at heel strike, as the force of impact sends shock waves through the soft tissues of the body [8]. In these types of abrupt situations, the frequency content of the artifact may overlap with that of the true muscle activity [9].

There has been considerable work to mitigate the effects of crosstalk, mostly through the continued development of advanced computer models. Merletti et al. showed the effects of motor unit characteristics on the surface EMG signal [10], [11], while Farina et al. developed a model that incorporates the nonhomogeneity of human muscle, fat and skin and used it to investigate the effects of source location on crosstalk [12], [13]. Lowery et al. also incorporated the complexities of the different human tissues into a finite-element model that demonstrated how differences in subcutaneous layers affect the level of EMG crosstalk [14]. Advanced filtering techniques have also been developed to identify and reduce crosstalk on experimental data [15], [16]. However, computer models are unable to distinguish between different EMG hardware, and filtering techniques are susceptible to the inherent variability of the EMG signal. For example, human EMG data during walking tends to be more variable for proximal and biarticular muscles [17]. Furthermore, reproducibility of human EMG data during running is highly dependent on the target muscle and the specific parameters of the EMG signal that are investigated [18].

In a similar way, motion artifacts have been addressed by researchers for decades, but there remain limitations in assessing technologies for removing motion artifacts. Researchers and organizations have suggested standards for appropriate signal filtering when using surface electrodes [19]. More recently, Thongpanja et al. developed a set of statistical descriptors for identifying EMG data contaminated with motion artifact by analyzing its probability density function [20]. However, as new technology is introduced for use in dynamic conditions, such as high-density EMG [21], it is imperative to consider the methods used for proper artifact rejection. To date, methods to eliminate motion artifact have been focused on surface recordings with bipolar electrodes. Based on the combined effects of crosstalk and motion artifact on new EMG technologies, it would be helpful to develop a method for assessing different surface EMG hardware and signal processing methods using known, ground-truth sources of data.

Manuscript received April 4, 2019; revised August 19, 2019; accepted September 22, 2019. Date of publication October 9, 2019; date of current version December 6, 2019. This work was supported by the Cognition and Neuroergonomics Collaborative Technology Alliance under Grant ARL W911NF-10-2-0022. *(Corresponding author: Bryan R. Schlink.)*

The authors are with the J. Crayton Pruitt Family Department of Biomedical Engineering, University of Florida, Gainesville, FL 32608 USA (e-mail: bschlink@ufl.edu; dferris@bme.ufl.edu).

Digital Object Identifier 10.1109/TNSRE.2019.2944297

One method to simulate EMG data is with an electrical leg phantom. Electrical phantom devices typically consist of a conductive material with embedded wires which can broadcast ground-truth electrical signals. A main advantage of a phantom is that it is relatively immune to the inherent variability of human EMG signals, as the same set of signals can be broadcast without changes due to fatigue, pain, etc. Furthermore, phantoms provide an objective method to assess different processing methods and measurement equipment [22]. Although computer models can simulate different physiological conditions of EMG recordings, they are unable to test the effects of different recording systems. Conversely, a phantom can provide a consistent, ground-truth set of signals that can be evaluated across many types of EMG systems. Phantoms have previously been used to simulate electrocortical data for the purposes of optimizing source localization and assessing different sources of artifact in electroencephalographic (EEG) recordings [23]–[26]. However, phantom devices have not been developed for to assess how crosstalk and motion artifact affect the performance of different EMG systems.

The purpose of this study was to design, build, and evaluate an electrical leg phantom with known, ground-truth muscle electrical sources. We wanted to demonstrate that such a phantom could provide a way to quantify crosstalk and motion artifact attenuation in EMG. Additionally, we wanted to show that these analyses were not limited to one type of EMG hardware, so we used different types of electrodes throughout our analyses. We developed a phantom consisting of antennae embedded in a conductive gelatin material and broadcast signals from these antennae to be recorded with EMG sensors at the phantom surface. We had three aims: (1) to characterize the relationship of the signals input to the antennae and the output recorded at the surface of the phantom; (2) to vary the amplitude of signals being broadcast through the phantom as a way to induce different levels of crosstalk between neighboring muscles; (3) to investigate the effects of motion artifact on the signal quality recorded with a high-density EMG array.

II. Methods

A. Phantom Design

We designed our leg phantom to be anatomically similar to that of an adult human shank. We used a 3D scanner (Artec Eva, Artec, Santa Clara, CA) to scan the left lower leg of a healthy adult male and then used this scan to form the mold for our phantom with 3D modeling software (Solidworks, Dassault Systems, Waltham, MA). We printed the mold using a 3D printer (Markforged, Watertown, MA); the mold was scaled to approximately 70% of the original size of the scan so that it fit on the printer bed. To provide stability for the phantom, we printed a human tibia and fibula from an open-source 3D model and attached them to a circular base (Fig. 1, left).

To create the antennae that broadcast electrical signals through the phantom, we ran 24 pairs of wires up through the base and tethered them to the tibia and fibula. The tips of each antenna were at a depth of 1-2 cm from the outer surface of the phantom, and we oriented the wires vertically to simulate the orientation of muscle fibers in the leg. We separated the antennae into four groups in the areas of the phantom that represent four major lower limb muscles: tibialis anterior, soleus, lateral gastrocnemius, and medial gastrocnemius. Finally, the soft tissues of the phantom were created using a mixture of ballistics gelatin, deionized water, and sodium chloride. This composition was chosen because it has comparable mechanical properties to human skin, fat, and muscle [27], [28]. Ballistics gelatin and human fat/muscle have a similar response to impact forces [29], [30], and it has been used as a surrogate for human tissues in several previous phantom designs [24], [31], [32].

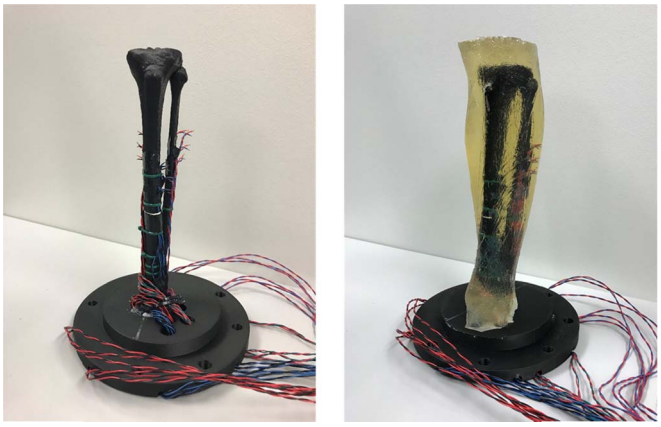

Fig. 1. Above pictures are anterior views of the phantom before (left) and after (right) the gelatin mixture was added to the mold and solidified. We divided twenty-four pairs of wires into four groups in the approximate areas of the tibialis anterior, soleus, lateral gastrocnemius, and medial gastrocnemius. We mixed sodium chloride with ballistics gelatin to simulate the conductive properties of human tissue.

B. Signal Generation

We transmitted two types of files to the phantom throughout the different phases of the experiment: (1) sinusoidal bursts generated using software (MATLAB, The Mathworks, Natick, MA) and (2) simulated EMG data created using an established model [33], [34]. Although our goal was a phantom that broadcast physiologically-relevant EMG signals, sinusoidal bursts allowed us to characterize aspects of phantom performance with a less complex signal. Fig. 2 shows a representative 2-second window for each of these signal types. The sinusoidal bursts had a frequency of 25 Hz and we varied their amplitudes throughout the experiment. The simulated EMG data were created using physiologically-relevant parameters for the human gastrocnemius during walking [35], [36]. We created two signals with different contraction times to simulate muscle activity during walking at different speeds. Custom-written scripts and data acquisition platforms (LabVIEW/National Instruments, Austin, TX, USA) transmitted both types of signals to the antennae of the phantom at a rate of 1000 Hz to be consistent with the pre-recorded EMG data.

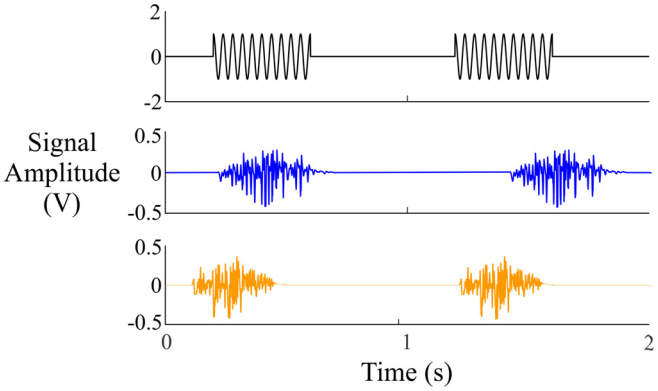

Fig. 2. We broadcast two types of files from the embedded antennae of the phantom. Sinusoidal bursts (top row; black) allowed us to characterize the relationship between the input and output signals of the phantom in a very reproducible way. We used simulated EMG data from the gastrocnemius (middle and bottom rows) to test more biologically complex signals.

C. Ground Electrode Resistance

We placed the phantom on a table at a safe distance from the DAQs and computers so that it would not record excessive electrical noise. The ground electrode was placed at the bottom of the phantom in an area without antennae broadcasting. We measured the resistance across the ground location with a handheld multimeter. We broadcast sinusoidal bursts with a peak-to-peak amplitude of 2V at a frequency of 25 Hz from one antenna of the phantom. We placed a bipolar EMG electrode on the phantom surface over this antenna location and recorded these sinusoidal bursts. Once this trial had been recorded, we removed the ground electrode. We then placed a small heat gun approximately six inches away from the ground location and blew air at room temperature on the ground location for fifteen minutes. We then measured the resistance across this area once again to confirm that drying the gel increased the resistance. To test the effects of a higher-resistance ground, we broadcast the same sinusoidal bursts as before and recorded using the same bipolar electrode in the same location. We compared the outputs from each of these trials (before and after drying) to see the effects on the signal amplitude.

D. Signal Input/Output Comparison

Previous research with electrical head phantoms in our lab has shown that the conductive material of the phantom leads to attenuation of the input signal from the antennae [22], [24], [25]. Therefore, we first needed to determine the appropriate adjustments to the input amplitudes in order to produce physiologically relevant recordings at the phantom surface. Physiologically relevant amplitudes were determined by comparing the phantom output amplitudes to the human EMG signals we previously recorded during walking and running. We broadcast sinusoidal bursts with peak-to-peak amplitudes ranging from 0.2 to 4 V in increments of 0.2 V and recorded the signals at the surface with bipolar EMG electrodes (Biometrics). Once we determined the input amplitudes that produced output amplitudes seen in human walking and running EMG, we scaled our pre-recorded EMG data to these levels.

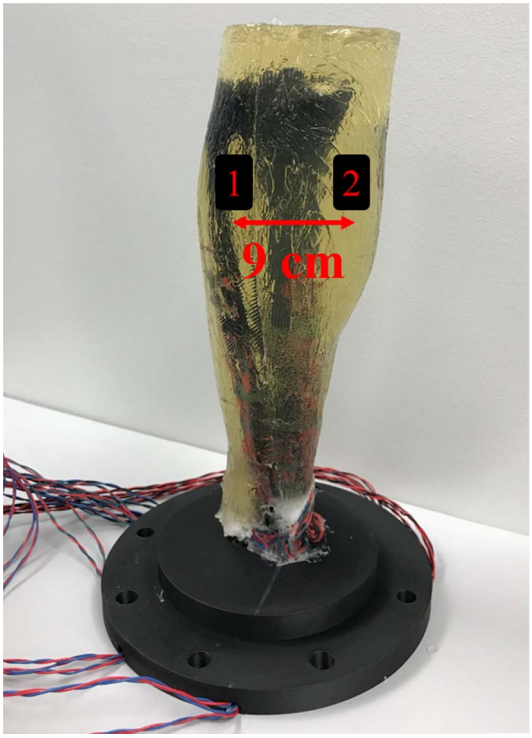

Fig. 3. We placed two recording electrodes ('1' and '2', above) on the surface of the phantom 9 cm apart to measure crosstalk. Two antenna (one underneath each electrode) simultaneously broadcast simulated EMG data from the lateral and medial gastrocnemii at varying amplitudes.

E. Crosstalk Induction and Measurement

To induce crosstalk between recording electrodes, we recorded from multiple sites while multiple signals were broadcast. We placed two bipolar surface electrodes (Biometrics) on the surface of the phantom directly over two antennae broadcasting signals (Figure 3; Electrode 1 was placed over Antenna 1, Electrode 2 over Antenna 2). The distance between Antenna 1 and Antenna 2 was approximately 9 cm. Antenna 1 broadcast simulated EMG data during walking from the lateral gastrocnemius for 10 seconds at a physiologically-relevant amplitude. Antenna 2 simultaneously broadcast simulated human EMG data during walking from the medial gastrocnemius.

We recorded several trials of surface EMG from the phantom while Antenna 1 and Antenna 2 broadcast their respective signals. Throughout all trials, Antenna 1's signal was kept constant. We then varied the broadcast amplitude levels of Antenna 2's signal (0.5, 1.0, 1.5 and 2x the broadcast amplitude of Antenna 1). To quantify the effects of crosstalk in each scenario, we calculated Pearson's correlation coefficient between Antenna 1 with no input from Antenna 2 and each level of Antenna 2 input.

F. Motion Artifact Analysis

To simulate the effects of motion artifact, we dropped the phantom from a short height above the table while simulated

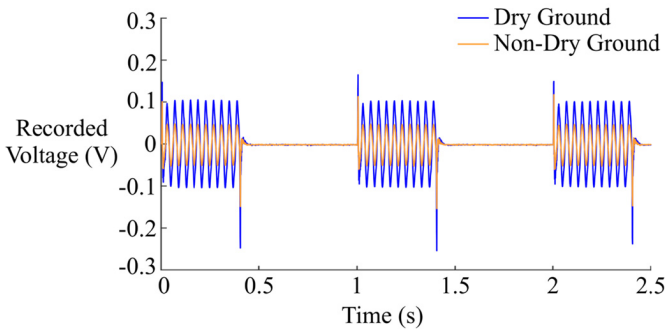

Fig. 4. We compared phantom surface recordings from sinusoidal bursts input before (orange) and after (blue) drying the ground location to increase its resistance. Output amplitudes were twice as high in the dry condition.

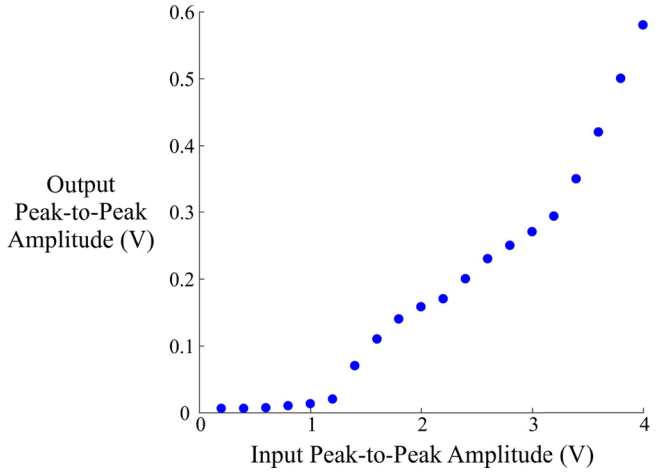

Fig. 5. We examined the relationship between the peak-to-peak amplitude of input sinusoidal bursts and the peak-to-peak amplitude of the signal recorded at the surface of the phantom. There was an overall nonlinear change in the gain between input and output amplitudes.

EMG data were broadcast from one antenna of the phantom. We recorded high-density surface EMG signals with a 64-channel array arranged in five columns of 13 electrodes (OT Bioelettronica, Turin, Italy). These 64 monopolar signals were converted to 59 differential signals along the longitudinal axis of the array. We then high-pass filtered the signals (20 Hz 4^{th}-order Butterworth) and calculated the average root mean square (RMS) value for all channels over the window that included the resulting motion artifact from the impact of the table and the closest burst of EMG activity. We also broadcast the same simulated EMG data and recorded signals at the surface while the phantom was stationary for comparison. To confirm that we introduced physiologically-relevant motion artifact in our recording, we compared the amplitude and frequency content from our phantom recording to a high-density recording from a healthy subject during treadmill running.

III. Results

The ground location had an original resistance of 180 kΩ prior to drying it out. After drying with air for 15 minutes, the resistance increased to 850 kΩ. We measured this resistance throughout our data collection and found a change of ±10 kΩ over time, indicating that the resistance was stable and the gel did not rehydrate to its previous level during the data collection. A higher resistance at the ground electrode led to higher amplitudes in surface recordings. Fig. 4 shows the sinusoidal bursts recorded at the phantom surface with and without drying the ground location. When the ground was dried and had a higher resistance (blue line), the signal was approximately twice as large as the signal when the ground was not dried (orange line).

The amplitude of the EMG signal at the phantom surface was reduced by approximately a factor of 10 when compared to the input amplitude (Fig. 5). At very low levels of sinusoidal amplitudes, the recorded signal was relatively indistinguishable from the baseline noise. Input signals with amplitudes between 1 and 3 V led to a nearly linear 1-to-1 relationship with the output signal. Larger input amplitudes (3.5+ V) also had a fairly linear relationship to the output signal, albeit at a steeper slope.

We were able to generate increasing levels of crosstalk between our recording electrodes as we increased the broadcast amplitude for Antenna 2 (Fig. 6, left). When Antenna 2 broadcast at lower amplitudes, the signal recorded from Electrode 1 closely resembled the true signal. However, increasing levels of Antenna 2 amplitude induced greater crosstalk, thereby reducing the similarity between the true Antenna 1 signal and the recorded signals (Fig. 6, bottom 2 rows). Pearson's correlation coefficient decreased sharply once the Antenna 2 amplitude was greater than its normal physiological value (Fig. 6, right).

When motion artifact was induced, the average RMS amplitude of several differential channels across the electrode array increased when compared to the stationary condition. High-pass filtering the data with a cutoff frequency of 20 Hz reduced, but did not eliminate, the motion artifact. Individual channel data showed a clear motion artifact before and after filtering the data (Fig. 7, top). As a result, the RMS values for many electrodes were higher with motion artifact compared to the same recording when the phantom was stationary (Fig. 7, bottom). The amplitude and frequency content of the recorded phantom data with motion artifact closely matched what is seen during running in human subjects, indicating that we simulated a reasonable representation of motion artifact seen in high-density EMG (Fig. 8).

IV. Discussion

We developed an electrical lower limb phantom capable of broadcasting physiological signals for the induction and analysis of EMG crosstalk and motion artifact. To our knowledge, this is the first and only electrical lower limb phantom for assessing EMG signals. We demonstrated that high-fidelity signals can be recorded with different types of surface EMG electrodes. Additionally, we were able to induce both crosstalk and motion artifact into our measurements, thereby providing a novel, ground-truth method for researchers to objectively assess their EMG hardware and processing techniques.

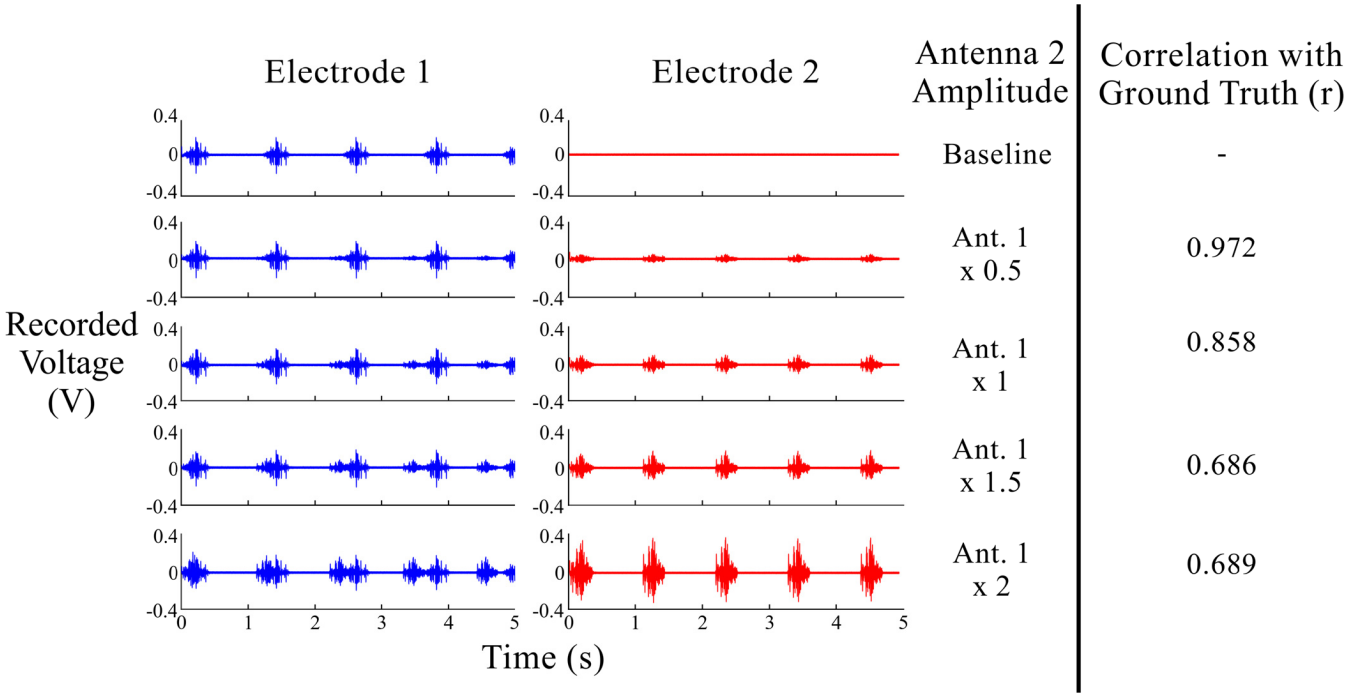

Fig. 6. At left, EMG recordings from the phantom surface at varying levels of Antenna 2 broadcast amplitude. We held the amplitude from Antenna 1 constant across all trials. At right, Pearson's correlation coefficient between the surface recording at Electrode 1 with no input from Antenna 2 (ground truth) and each level of Antenna 2 input.

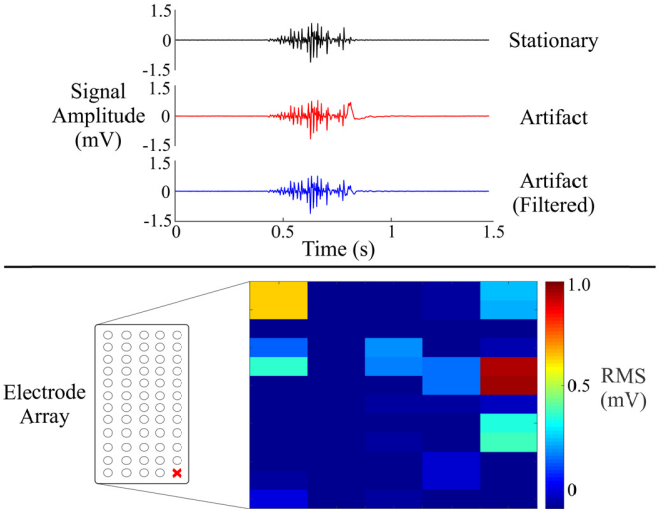

Fig. 7. At top, a representative channel from the high-density EMG array during the stationary condition (black) as well as during the motion artifact condition before (red) and after high-pass filtering the data (blue). At bottom, difference of RMS values between recordings when motion artifact was induced and when the phantom was stationary for all differential electrodes of the high-density array. Positive RMS values indicate that signal was higher with motion artifact.

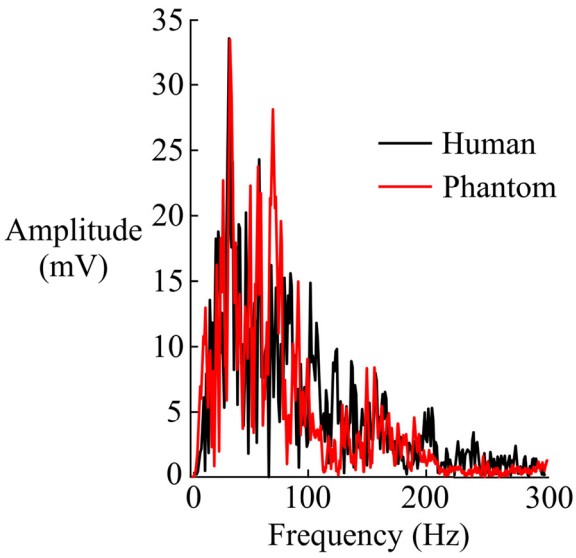

Fig. 8. Amplitude and frequency content for a representative channel from a high-density EMG recording in two conditions: (1) a human subject running at 5.0 m/s (black) and (2) our motion artifact simulation with the phantom (red). The similarities in amplitude at frequencies typically associated with motion artifacts (<100 Hz) showed that our simulated artifacts were a relatively accurate representation of real artifacts seen during running.

Reducing the resistance at the ground location was a beneficial step in our recordings, and it mirrored proper human EMG recording technique. In a bipolar recording, the signal from the ground electrode is subtracted from the difference in signal between the two recording electrodes [37]. Therefore, it is imperative that the ground electrode contain no portion of the actual signal being recorded. This is normally accomplished by placing the electrode on a bony prominence near the recording site. Although this was not available to us, drying out the ground location increased the resistance by nearly a factor of five while still keeping it within the physiological range of resistance for human skin [38]. As such, we were

able to record signals with approximately twice the amplitude compared to recordings taken without drying the ground location.

We successfully induced crosstalk between surface electrodes placed over separate sources in the phantom. In doing so, we've provided a method for researchers to test new techniques for crosstalk removal, such as blind signal separation [39] or double differential [13] and branched electrode configurations [40]. To date, these methods have all been tested with either computer simulations or human EMG data. Simulations often do not include the conductive properties of human tissue [13], which may affect the conduction velocity of action potentials [41]. On the other hand, human EMG measurements can vary based on experimental aspects, such as electrode location [42]. Intersubject variability also plays a role, as muscle size and tissue volume can make it difficult to compare processing methods across subjects [43]. However, our phantom eliminates these concerns by using ground-truth measurements to determine the level of crosstalk. Since we know the exact characteristics of the signals input to the phantom, we are able to accurately assess the level of contamination in the output signal.

One limitation of our phantom design was that it was a continuous, homogenous medium. It had consistent conductance and resistivity values throughout the entire phantom. Human tissues (muscle, fat, skin, etc.) have varying levels of resistivity which affect the conductance of electrical signal from the neuromuscular junction to the point at which it is measured at the skin surface [44]. However, we were able to successfully characterize the input/output relationship and produce signals at the surface that resembled human EMG data in both amplitude and shape. This is a significant improvement in comparison to other recently developed phantoms that exclusively broadcast non-physiological data [22], [24] and the next logical progression in phantom development. Future phantoms should incorporate a multi-layer design that would provide a more physiologically-accurate representation for EMG signal simulation. This could be accomplished by varying the proportions of ballistics gelatin and sodium chloride to create layers with different conductance properties [45]. Materials with different conductivities, such as dental plaster, agar, or synthetic polymers [46], could also be layered to simulate different tissues and add complexity to the phantom. Researchers should then characterize the impedance of the phantom and see how it changes with different signal frequencies and source locations. Additionally, motion artifacts are typically generated by the movement of the muscle below the skin during a contraction and force impulses that cause movement at the electrode-skin interface during movement [19]. Each of these sources of artifact changes the geometry of the recording site. Although our phantom is composed of soft, deformable material, it likely does not deform in the exact same manner that human tissue would during movement.

A more advanced leg phantom would also be beneficial for detecting motor unit firing patterns. We limited our signal broadcast to 1-2 antennae in each of the conditions we tested for simplicity. To simulate individual motor unit activity, more antennae should simultaneously broadcast physiological data to generate the EMG waveform at the surface. Although our phantom contained 24 antennae, this is much smaller than the actual number of motor units found in human muscle [47]. It would be useful to design future models with even smaller antennae so that the phantom can broadcast more signals. To this end, microelectrode arrays [48] could be converted to antennae, thereby creating a higher-density phantom. Precise simulation of motor unit discharge patterns would also help evaluate different methods of motor unit identification [49]–[51]. Spatial filtering, template matching techniques, mixing models, and convolutive decomposition methods are all methods to process high-density EMG data and determine motor unit discharge patterns [52]. Currently, there is no experimental ground-truth method for assessing the validity of these procedures. Intramuscular EMG is considered the gold standard for measuring and evaluating decomposition methods [49]. A high-density lower leg phantom could be used to test the different methods of decomposition and evaluate their effectiveness. Furthermore, these methods can be tested in both stationary and dynamic conditions. High-density EMG has been used to detect motor units in stationary conditions [52], but similar methods for use during dynamic conditions have yet to be developed. Our leg phantom may provide a practical, repeatable approach to develop and evaluate novel methods of motor unit detection during walking and running.

High-density EMG is a useful technique that has been used to quantify motor unit recruitment in a wide range of clinical applications [21]. Bipolar EMG is limited to a single recording site on a muscle, and slight changes in electrode location may lead to very different interpretations of muscle activity [53]. Conversely, high-density EMG allows researchers to map a muscle's spatial properties for a more detailed analysis [54]. Although it is traditionally used during stationary tasks, researchers have been trying to use it in dynamic conditions. Schmitz et al. measured quadriceps activity during stationary cycling [55], while Cronin et al. recorded high-density EMG activity during level walking at a self-selected speed [56]. Each of these studies demonstrated the utility of high-density EMG, and it can be applied in a wealth of basic science and clinical applications. Motion artifact was likely limited in each case due to small, or nonexistent, impact forces of the lower limbs. Our analysis of motion artifact showed that it was challenging to remove artifacts with standard bandpass filter measures. Furthermore, we observed an increase in RMS amplitude values at several electrode sites, indicating that motion artifact will likely affect multiple areas of the electrode array. Improving both the hardware and signal processing methods of high-density EMG can increase its use for a broader range of dynamic conditions. Our leg phantom provides an objective way to compare different processing techniques with ground truth measurements. Future phantoms could provide more robust documentation and validation of different high-density EMG hardware and signal processing approaches.

ACKNOWLEDGMENTS

The authors would like to thank Dr. A. Nordin for his assistance in the design of the phantom and the development of the

files broadcast through the phantom, as well as M. MacLean for her assistance with the 3D printing of the phantom mold and components.

REFERENCES

[1] E. Criswell, *Cram's Introduction to Surface Electromyography*. Burlington, MA, USA: Jones & Bartlett, 2011.

[2] C. J. De Luca, "The use of surface electromyography in biomechanics," *J. Appl. Biomech.*, vol. 13, no. 2, pp. 135–163, May 1997.

[3] D. Farina, R. Merletti, and R. M. Enoka, "The extraction of neural strategies from the surface EMG," *J. Appl. Physiol.*, vol. 96, no. 4, pp. 1486–1495, 2004.

[4] D. A. Winter, A. J. Fuglevand, and S. E. Archer, "Crosstalk in surface electromyography: Theoretical and practical estimates," *Kinesiology*, vol. 4, no. 1, pp. 15–26, 1994.

[5] J. P. M. Mogk and P. J. Keir, "Crosstalk in surface electromyography of the proximal forearm during gripping tasks," *J. Electromyogr. Kinesiol.*, vol. 13, pp. 63–71, Feb. 2003.

[6] C. J. De Luca and R. Merletti, "Surface myoelectric signal cross-talk among muscles of the leg," *Electroencephalogr. Clin. Neurophysiol.*, vol. 69, no. 6, pp. 568–575, Jun. 1988.

[7] E. A. Clancy, E. L. Morin, and R. Merletti, "Sampling, noise-reduction and amplitude estimation issues in surface electromyography," *J. Electromyograph. Kinesiol.*, vol. 12, no. 1, pp. 1–16, Feb. 2002.

[8] J. M. Wakeling, A.-M. Liphardt, and B. M. Nigg, "Muscle activity reduces soft-tissue resonance at heel-strike during walking," *J. Biomech.*, vol. 36, pp. 1761–1769, Dec. 2003.

[9] R. Merletti and D. Farina, *Surface Electromyography: Physiology, Engineering, and Applications*. Hoboken, NJ, USA: Wiley, 2016.

[10] R. Merletti, L. L. Conte, E. Avignone, and P. Guglielminotti, "Modeling of surface myoelectric signals. I. Model implementation," *IEEE Trans. Biomed. Eng.*, vol. 46, no. 7, pp. 810–820, Jul. 1999.

[11] R. Merletti, S. H. Roy, E. Kupa, S. Roatta, and A. Granata, "Modeling of surface myoelectric signals. II. Model-based signal interpretation," *IEEE Trans. Biomed. Eng.*, vol. 46, no. 7, pp. 821–829, Jul. 1999.

[12] D. Farina and R. Merletti, "A novel approach for precise simulation of the EMG signal detected by surface electrodes," *IEEE Trans. Biomed. Eng.*, vol. 48, no. 6, pp. 637–646, Jun. 2001.

[13] D. Farina, R. Merletti, B. Indino, M. Nazzaro, and M. Pozzo, "Surface EMG crosstalk between knee extensor muscles: Experimental and model results," *Muscle Nerve*, vol. 26, no. 5, pp. 681–695, 2002.

[14] M. M. Lowery, N. S. Stoykov, A. Taflove, and T. A. Kuiken, "A multiple-layer finite-element model of the surface EMG signal," *IEEE Trans. Biomed. Eng.*, vol. 49, no. 5, pp. 446–454, May 2002.

[15] X. Zhang and P. Zhou, "Filtering of surface EMG using ensemble empirical mode decomposition," *Med. Eng. Phys.*, vol. 35, no. 4, pp. 537–542, 2013.

[16] L. Mesin, "Optimal spatio-temporal filter for the reduction of crosstalk in surface electromyogram," *J. Neural Eng.*, vol. 15, no. 1, Feb. 2018, Art. no. 016013.

[17] D. A. Winter and H. J. Yack, "EMG profiles during normal human walking: Stride-to-stride and inter-subject variability," *Electroencephalogr. Clin. Neurophysiol.*, vol. 67, no. 5, pp. 402–411, 1987.

[18] K. Karamanidis, A. Arampatzis, and G.-P. Brüggemann, "Reproducibility of electromyography and ground reaction force during various running techniques," *Gait Posture*, vol. 19, pp. 115–123, Apr. 2004.

[19] C. J. De Luca, L. D. Gilmore, M. Kuznetsov, and S. H. Roy, "Filtering the surface EMG signal: Movement artifact and baseline noise contamination," *J. Biomech.*, vol. 43, no. 8, pp. 1573–1579, 2010.

[20] S. Thongpanja, A. Phinyomark, F. Quaine, Y. Laurillau, C. Limsakul, and P. Phukpattaranont, "Probability density functions of stationary surface EMG signals in noisy environments," *IEEE Trans. Instrum. Meas.*, vol. 65, no. 7, pp. 1547–1557, Jul. 2016.

[21] G. Drost, D. F. Stegeman, B. G. M. van Engelen, and M. J. Zwarts, "Clinical applications of high-density surface EMG: A systematic review," *J. Electromyogr. Kinesiol.*, vol. 16, pp. 586–602, Dec. 2006.

[22] A. S. Oliveira, B. R. Schlink, W. D. Hairston, P. König, and D. P. Ferris, "Induction and separation of motion artifacts in EEG data using a mobile phantom head device," *J. Neural Eng.*, vol. 13, no. 3, May 2016, Art. no. 036014.

[23] R. M. Leahy, J. C. Mosher, M. E. Spencer, M. X. Huang, and J. D. Lewine, "A study of dipole localization accuracy for MEG and EEG using a human skull phantom," *Electroencephalogr. Clin. Neurophysiol.*, vol. 107, no. 2, pp. 159–173, Apr. 1998.

[24] E.-R. Symeonidou, A. D. Nordin, W. D. Hairston, and D. P. Ferris, "Effects of cable sway, electrode surface area, and electrode mass on electroencephalography signal quality during motion," *Sensors*, vol. 18, no. 4, p. 1073, 2018.

[25] S. M. Peterson and D. P. Ferris, "Combined head phantom and neural mass model validation of effective connectivity measures," *J. Neural Eng.*, vol. 16, no. 2, Apr. 2019, Art. no. 026010.

[26] J. Zhang *et al.*, "A novel 3D-printed head phantom with anatomically realistic geometry and continuously varying skull resistivity distribution for electrical impedance tomography," *Sci. Rep.*, vol. 7, no. 1, Dec. 2017, Art. no. 4608.

[27] A. I. Farrer *et al.*, "Characterization and evaluation of tissue-mimicking gelatin phantoms for use with MRgFUS," *J. Ther. Ultrasound*, vol. 3, no. 1, p. 9, Dec. 2015.

[28] T. F. Juliano, A. M. Forster, P. L. Drzal, T. Weerasooriya, P. Moy, and M. R. VanLandingham, "Multiscale mechanical characterization of biomimetic physically associating gels," *J. Mater. Res.*, vol. 21, no. 8, pp. 2084–2092, Aug. 2006.

[29] T. Payne, S. Mitchell, R. Bibb, and M. Waters, "The evaluation of new multi-material human soft tissue simulants for sports impact surrogates," *J. Mech. Behav. Biomed. Mater.*, vol. 41, pp. 336–356, Jan. 2015.

[30] D. S. Cronin and C. Falzon, "Characterization of 10% ballistic gelatin to evaluate temperature, aging and strain rate effects," *Exp. Mech.*, vol. 51, no. 7, pp. 1197–1206, Sep. 2011.

[31] W. D. Hairston, G. A. Slipher, and A. B. Yu, "Ballistic gelatin as a putative substrate for EEG phantom devices," 2016, *arXiv:1609.07691*. [Online]. Available: https://arxiv.org/abs/1609.07691

[32] N. Richer, R. J. Downey, A. D. Nordin, W. D. Hairston, and D. P. Ferris, "Adding neck muscle activity to a head phantom device to validate mobile EEG muscle and motion artifact removal," in *Proc. 9th Int. IEEE/EMBS Conf. Neural Eng. (NER)*, Mar. 2019, pp. 275–278.

[33] A. J. Fuglevand, D. A. Winter, A. E. Patla, and D. Stashuk, "Detection of motor unit action potentials with surface electrodes: Influence of electrode size and spacing," *Biol. Cybern.*, vol. 67, no. 2, pp. 143–153, Jun. 1992.

[34] A. J. Fuglevand, D. A. Winter, and A. E. Patla, "Models of recruitment and rate coding organization in motor-unit pools," *J. Neurophysiol.*, vol. 70, no. 6, pp. 2470–2488, Dec. 1993.

[35] B. Feinstein, B. Lindegård, E. Nyman, and G. Wohlfart, "Morphologic studies of motor units in normal human muscles," *Cells Tissues Organs*, vol. 23, no. 2, pp. 127–142, 1955.

[36] S. Leahy, C. Toomey, K. McCreesh, C. O'Neill, and P. Jakeman, "Ultrasound measurement of subcutaneous adipose tissue thickness accurately predicts total and segmental body fat of young adults," *Ultrasound Med. Biol.*, vol. 38, no. 1, pp. 28–34, Jan. 2012.

[37] G. Kamen and D. Gabriel, *Essentials of Electromyography*. Champaign, IL, USA: Human Kinetics, 2010.

[38] J. G. Webster and J. W. Clark, *Medical Instrumentation: Application and Design*. Hoboken, NJ, USA: Wiley, 1995.

[39] J. M. Kilner, S. N. Baker, and R. N. Lemon, "A novel algorithm to remove electrical cross-talk between surface EMG recordings and its application to the measurement of short-term synchronisation in humans," *J. Physiol.*, vol. 538, no. 3, pp. 919–930, Feb. 2002.

[40] B. C. Fortune, L. R. McKenzie, L. T. Chatfield, and C. G. Pretty, "Crosstalk reduction in forearm electromyography during static gripping," in *Proc. 14th IEEE/ASME Int. Conf. Mechatronic Embedded Syst. Appl. (MESA)*, Jul. 2018, pp. 1–6.

[41] J. Schneider, J. Silny, and G. Raul, "Influence of tissue inhomogeneities on noninvasive muscle fiber conduction velocity measurements-investigated by physical and numerical modeling," *IEEE Trans. Biomed. Eng.*, vol. 38, no. 9, pp. 851–860, Sep. 1991.

[42] J.-Y. Hogrel, J. Duchêne, and J.-F. Marini, "Variability of some SEMG parameter estimates with electrode location," *J. Electromyogr. Kinesiol.*, vol. 8, no. 5, pp. 305–315, Oct. 1998.

[43] T. J. Koh and M. D. Grabiner, "Cross talk in surface electromyograms of human hamstring muscles," *J. Orthopaedic Res.*, vol. 10, no. 5, pp. 701–709, Sep. 1992.

[44] L. A. Geddes and L. E. Baker, "The specific resistance of biological material—A compendium of data for the biomedical engineer and physiologist," *Med. Biol. Eng.*, vol. 5, no. 3, pp. 271–293, May 1967.

[45] M. A. Kandadai, J. L. Raymond, and G. J. Shaw, "Comparison of electrical conductivities of various brain phantom gels: Developing a 'brain gel model,'" *Mater. Sci. Eng. C, Mater. Biol. Appl.*, vol. 32, no. 8, pp. 2664–2667, Dec. 2012.

[46] A. Hellerbach, V. Schuster, A. Jansen, and J. Sommer, "MRI phantoms–are there alternatives to agar?" *PLoS ONE*, vol. 8, no. 8, 2013, Art. no. e70343.

[47] A. J. McComas, P. R. Fawcett, M. J. Campbell, and R. E. Sica, "Electrophysiological estimation of the number of motor units within a human muscle," *J. Neurol. Neurosurg. Psychiatry*, vol. 34, no. 2, pp. 121–131, Apr. 1971.

[48] P. R. Patel *et al.*, "Chronic *in vivo* stability assessment of carbon fiber microelectrode arrays," *J. Neural Eng.*, vol. 13, no. 6, Dec. 2016, Art. no. 066002.

[49] D. Farina, A. Holobar, R. Merletti, and R. M. Enoka, "Decoding the neural drive to muscles from the surface electromyogram," *Clin. Neurophysiol.*, vol. 121, no. 10, pp. 1616–1623, Oct. 2010.

[50] A. Holobar, D. Farina, M. Gazzoni, R. Merletti, and D. Zazula, "Estimating motor unit discharge patterns from high-density surface electromyogram," *Clin. Neurophysiol.*, vol. 120, no. 3, pp. 551–562, 2009.

[51] A. Holobar, M. A. Minetto, and D. Farina, "Accurate identification of motor unit discharge patterns from high-density surface EMG and validation with a novel signal-based performance metric," *J. Neural Eng.*, vol. 11, no. 1, Feb. 2014, Art. no. 016008.

[52] R. Merletti, A. Holobar, and D. Farina, "Analysis of motor units with high-density surface electromyography," *J. Electromyogr. Kinesiol.*, vol. 18, pp. 879–890, Dec. 2008.

[53] J. A. Mercer, N. Bezodis, D. DeLion, T. Zachry, and M. D. Rubley, "EMG sensor location: Does it influence the ability to detect differences in muscle contraction conditions?" *J. Electromyogr. Kinesiol.*, vol. 16, no. 2, pp. 198–204, Apr. 2006.

[54] B. G. Lapatki, J. P. van Dijk, I. E. Jonas, M. J. Zwarts, and D. F. Stegeman, "A thin, flexible multielectrode grid for high-density surface EMG," *J. Appl. Physiol.*, vol. 96, no. 1, pp. 327–336, Jan. 2004.

[55] J. P. J. Schmitz, J. P. van Dijk, P. A. J. Hilbers, K. Nicolay, J. A. L. Jeneson, and D. F. Stegeman, "Unchanged muscle fiber conduction velocity relates to mild acidosis during exhaustive bicycling," *Eur. J. Appl. Physiol.*, vol. 112, pp. 1593–1602, May 2012.

[56] N. J. Cronin, S. Kumpulainen, T. Joutjarvi, T. Finni, and H. Piitulainen, "Spatial variability of muscle activity during human walking: The effects of different EMG normalization approaches," *Neuroscience*, vol. 300, pp. 19–28, Aug. 2015.